Journal of Low Temperature Physics, Vol. 27, Nos. 5/6, 1977

Review Paper: "Brute-Force" Nuclear Orientation: A Survey of Accomplishments and Problems to Date*†

William D. Brewer

Fachbereich Physik der Freien Universität Berlin, West Germany

(Received November 4, 1976)

The technique of "brute-force" or direct low-temperature nuclear orientation has become practicable since about 1970 with the development of cryostats capable of producing the required combination of fields and temperatures. This is reflected in the increasing number of experiments reported in recent years. We summarize here the potential applications and some of the initial difficulties of the technique. New data for the systems ^{95}*Ta*Ta, ^{110}*Ag*^{m}Ag *and Co*Mo *are presented, and the results of a magnetic resonance experiment on* ^{95}*Nb nuclei oriented by the direct method are compared with data from a conventional resonance experiment in Fe host.*

1. INTRODUCTION

The "brute-force" or direct method of orienting nuclei at low temperatures is the oldest and, for practitioners of nuclear orientation, has long been one of the most fascinating techniques. It was first suggested in 1934,[1,2] shortly after the first measurements of nuclear magnetic moments appeared. In the brute-force orientation method (BFO), the nuclear magnetic sublevels are split by the application of an external magnetic field H, and the nuclear spin temperature is lowered by establishing thermal equilibrium with a suitable thermal reservoir, so that population differences, given by the Boltzmann distribution, appear between the sublevels. Such an ensemble of oriented nuclei can be described by statistical tensors B_k^q,[3] which are functions of the sublevel splitting Δ and the thermal energy $k_B T$. If the interaction that produces Δ has cylindrical symmetry (as is always the case in BFO), the set of $2I+1$ components B_k^0 suffices to describe the orientation

* This paper is based on a summary talk given at the EPS Study Conference on Nuclear Orientation, Oxford, July 1976.

† Supported in part by Deutsche Forschungsgemeinschaft (SFB 161).

completely, where I is the nuclear spin and k takes on integral values from 0 to $2I$. Historically, an orientation described by B_1 (dropping the superfluous index q) was termed polarization (or magnetization); it shows forward–backward asymmetry with respect to the cylinder axis. The orientation described by B_2 is symmetric around the cylinder axis and is termed alignment. Only these two tensor components are important in BFO, since all higher components are extremely small at achievable field–temperature combinations.

2. APPLICATIONS OF BRUTE-FORCE ORIENTATION

2.1. General Considerations

The determining parameter in a BFO experiment, given a particular value of the nuclear spin and moment, is the field/temperature ratio H/T, conveniently expressed in tesla/kelvin. Because of the smallness of the nuclear magneton, rather large H/T values are required to produce an appreciable degree of orientation (i.e., B_1 or B_2 of order 0.1). Since B_1 increases as H/T, while B_2 increases as $(H/T)^2$, it is in fact easier to produce a detectable polarization. The degree of orientation needed depends of course on the particular application and/or the detection method. Several broad classes of applications are listed below.

Probably the earliest and certainly still the most widespread application of BFO is to produce the nuclear magnetization needed for a nuclear magnetic resonance (NMR) experiment. Here the applied field is usually in the range 2–10 T and temperatures between 1 K and room temperature or above are used, so that relatively modest values of H/T between 0.01 and 10 T/K are obtained, with consequently small degrees of nuclear polarization. In recent years BFO combined with NMR has been used for thermometry in fields of up to 1 T and temperatures down to the mK range.[4]

Perhaps the most straightforward application of BFO is its use in nuclear cooling, which dates back about 20 years but has only recently been very successful as a refrigeration method. Here large nuclear magnetizations are needed in order to provide sufficient entropy for subsequent cooling. Currently used H/T values are around 500 T/K.[5]

The direct determination of the nuclear susceptibility produced by BFO for low-temperature thermometry has also been reported.[6] This method is limited by the sensitivity of the magnetometer and by the paramagnetic signal from impurities in the sample. The use of SQUID magnetometers may extend its applicability and make it an attractive thermometer for some uses.

Nuclear orientation can also be detected by observing the scattering of polarized particles from polarized target nuclei. The BFO method has been used to produce such polarized targets for about 20 years and many experiments using polarized neutrons to investigate the nuclear force have been performed.[7] More recently, experiments with polarized meson beams have been undertaken.[8]

All of the above applications involve the polarization of stable nuclei. Another class of experiments, which uses detection of nuclear radiations emitted from radioactive nuclei, and which often requires nuclear alignment, is the main topic of this paper. In general there are three ways in which nuclear radiation can be used to detect nuclear orientation:

(i) Angular distribution measurements, in which the nuclear radiation-intensity distribution around the orientation axis is measured. Such experiments have been performed using β particles, γ rays, conversion electrons, α particles, fission fragments, and inner bremsstrahlung (IB) emitted by decaying nuclei. Due to parity conservation, only nuclear alignment can be detected, except for the case of β particles or IB. To date, only γ rays have been used extensively in BFO work, although the feasibility of using β-particle detection with BFO has been demonstrated.[9]

(ii) Measurements of circular or linear polarization of emitted radiations. This type of measurement (CP) is sensitive to the nuclear polarization, but involves a scattering process as part of the radiation detector and thus gives poor counting statistics. Its use in conjunction with BFO will probably be limited.

(iii) Direct energy resolution of the multipole components of emitted radiations. This is possible only with γ rays (Mössbauer effect) and is limited to certain suitable nuclei. It is sensitive to nuclear polarization and may well be used in combination with BFO, although many Mössbauer nuclei have relatively small magnetic moments, making BFO difficult.

2.2. Gamma-Ray Experiments

In the following, attention will be concentrated on angular distribution measurements of γ rays. As noted above, for this type of experiment a nuclear alignment is necessary. In most cases this means that a B_2 value of 0.1 or more is needed; for typical nuclear g-factors an H/T value greater than 450 T/K is then required (e.g., 9 T at 20 mK).

The intensity distribution of radiation from an axially symmetric ensemble of oriented nuclei is given by the formula

$$W(\theta) = 1 + \sum_k F_k U_k B_k(\beta) P_k (\cos\theta) \tag{1}$$

Here $W(\theta)$ is the normalized intensity at angle θ to the symmetry axis and k is an even integer from 2 to k_{max} for γ radiation, where k_{max} is the smaller of $2I'$ or $2L$ (I' is the smallest nuclear spin preceding the observed transition, L is the transition multipolarity). The P_k are Legendre polynomials of rank k, the U_k are coefficients which allow for reorientation in unobserved transitions (exactly calculable if the nuclear decay scheme is known), and the F_k are distribution coefficients, which for γ rays are identical with tabulated angular correlation coefficients.[10] By suitable modification of the F_k (and inclusion of odd k values for β decay), this formula can be made to apply to any type of nuclear radiation. The P_k must be corrected for the finite solid angle subtended by the radiation detector; this is done by multiplying with coefficients Q_k. The B_k are the previously mentioned orientation tensors; for BFO we have for the energy splitting

$$\Delta = -g\mu_N H, \qquad \beta = \Delta/k_B T \tag{2}$$

and, for small H/T or β values,[3]

$$\begin{aligned} B_1 &\approx [I(I+1)(2I+1)/3]\beta \\ B_2 &\approx \{[I(I+1)(2I-1)(3I+1)]^{1/2}/(6\sqrt{5})\}\beta^2 \end{aligned} \tag{3}$$

where g is the nuclear g-factor, μ_N is the nuclear magneton, β is the ratio of sublevel splitting to thermal energy, and I is the spin of the oriented nuclear state. The parameter β has the numerical value

$$\beta = 3.7 \times 10^{-4} gH/T\,[\mathrm{T/K}] \tag{4}$$

The B_k have been tabulated[11] for various values of β and I.

2.3. Specific Applications

Assuming that the required H/T value can be obtained, the following applications for BFO can be envisioned:

1. *Nuclear Physics.* Nuclear orientation has contributed in the past to the elucidation of decay schemes and determination of g factors. The particular advantage of BFO is that it is in principle universal—any nucleus with a nonzero moment can be oriented. No restrictions are placed on the composition of the source, and the nuclei may often be generated by a nuclear reaction in situ. The chemical and physical properties of the element studied are relatively unimportant. Finally, the nuclear interaction Hamiltonian is simple and provides no obstacle to interpreting the data. A BFO experiment could give information on decay schemes and a rough determination of the g-factor; for higher accuracy, NMR can be performed on the oriented nuclei (BF/NMR). In this case, g-factors of radioactive nuclei

could be measured with four-place accuracy (which may be useful in some cases as a calibration for other NMR experiments and in others for a detailed comparison of nuclei with similar structure). Also, hyperfine anomalies could be studied with the necessary precision.

2. *Solid State Physics.* In fact, a pure BFO experiment can probably never be carried out. The requirement of thermal equilibrium with a heat bath means that at least a dynamic hyperfine interaction of the nuclei must exist, giving a finite nuclear relaxation time T_1 to the host lattice. It is particularly important that T_1 not become too long at low temperatures. In most cases a small, static hyperfine interaction will also be present, leading to a shift of the applied field (chemical shift, Knight shift), or to an electric quadrupole splitting. It has been suggested by Stone[12] that observation of a perturbation of the BFO may be a sensitive way to detect such small interactions. Especially in the case of a BF/NMR experiment, they could be determined very accurately (although a separate Knight shift determination can only be made if the nuclear g-factor is known). The BFO technique permits the use of host–impurity combinations and of impurity concentrations that are inaccessible to most other methods, and should permit, e.g., the study of defect–impurity interactions at very low concentrations. Most experiments will probably be done in metals because of the thermal-contact requirement at low temperatures, although a thin film of an ionic crystal, a glass, or a frozen rare gas might also be feasible.

Because a residual hyperfine interaction is usually present, the question arises as to the practical definition of a brute-force experiment. In the following, any nuclear orientation measurement in which the external field is the *principal* source of the nuclear energy splitting Δ (i.e., other interactions are a factor of two or more smaller than the nuclear Zeeman splitting) will be classified as brute-force orientation.

3. *Thermometry.* Clearly the BFO method offers advantages as a nuclear thermometer if the required magnetic field can be tolerated. It is independent of separate determinations of hyperfine constants (but requires knowledge of the nuclear moment), requires no external connections to the cryostat working space, can be carried out with a variety of isotopes, permitting simultaneous measurements from several thermometers, requires only a very small mass for the thermometer (in principle nanograms), and its sensitivity can be adjusted to the temperature range by varying the magnetic field without otherwise affecting the measurement. This application has been explored at Leyden[13] and will be discussed further below.

4. *Methodology.* Because of the smallness of hyperfine perturbations in a BF/NMR experiment, the resonance lines should be very narrow, without the inhomogeneous broadening characteristic of ferromagnetic hosts.

Besides improving the accuracy of resonance measurements, this should permit the study of the resonance process itself without the complications of extremely broad lines.[14] Studies of multipole structure, skin effect, adiabatic fast passage response, and pulsed-NMR techniques on extremely dilute spin systems should be possible.

3. LIMITATIONS OF BFO

Without having actually carried out a BFO experiment, one can compile a list of a priori limitations which might be expected to apply to the method. Such limitations will be discussed in this section and later re-examined in the light of experimental results.

3.1. H/T Values

The most obvious problem in a BFO or BF/NMR experiment is attaining the necessary H/T value. The first experiments on polarized targets for neutron scattering used H/T values near 25 T/K. Improvements to the apparatus increased this value to about 50 T/K in a few years but only with the development of superconducting magnets in the 1960s did a quantum jump in available H/T values occur, making possible γ-ray anisotropy measurements on a variety of nuclei for the first time. Currently available apparatus (e.g., a conventional Nb–Ti solenoid giving $H \leq 9$ T and a ^{3}He/^{4}He dilution refrigerator yielding $T \geq 12$ mK) make possible H/T values in the range 700–800 T/K although most experiments to date have been performed at $H/T \leq 500$ T/K. New techniques include ultra-low-temperature dilution refrigerators,[15] Pomeranchuk cooling,[16] hyperfine-enhanced nuclear demagnization,[17] and direct nuclear demagnetization,[18] which give the possibility of temperatures in the 3–4 mK range for long time periods or in the 0.5 mK range for 24 h or more. Most of these techniques have been developed for the study of ^{3}He, but their application to nuclear orientation should present no problems in principle. At the same time, magnet technology has improved, so that superconducting solenoids giving upward of 17 T are now available and H/T values in excess of 5000 T/K may soon be feasible. At present, it is probably more economical to attempt to increase H/T by lowering the sample temperature rather than by raising the field, but this introduces new problems, as will be discussed below and in Section 4.

3.2. Uncertainties in the Nuclear Hamiltonian

One of the main advantages of the BFO method, particularly for nuclear physics applications, is that the nuclear level splitting is simply given

by the Zeeman interaction with the external field. As pointed out in Section 2.3, this ideal situation is in practice seldom realized, so that small magnetic and electric perturbations to the nuclear Hamiltonian must be taken into account. This is especially true if there are chemical or solubility problems in the source preparation or if a high defect concentration (e.g., from radiation damage) is present. If a resonance experiment is performed, the electric quadrupole interaction will be detectable as line broadening or splitting. A Knight shift, however, will be hard to detect unless the samples are inhomogeneous, with several impurity sites giving rise to variously shifted lines, or unless the g-factor is already known.

Another, in principle trivial, limitation is precise knowledge of the applied field H. In particular, in a BF/NMR experiment provision must be made for (preferably simultaneous) determination of H by NMR or some other precise method.

3.3. Thermometry

For the interpretation of BFO experiments, accurate thermometry in the millikelvin range in high applied fields is necessary. "Internal" thermometry by addition of an isotope with known nuclear properties, as is often used in nuclear orientation experiments with ferromagnetic hosts, is probably the best solution in the long run; for the present, most experiments have been done using a separate, ferromagnetic nuclear thermometer (see Section 4.2). Thermometry problems may be divided into two classes:

(i) Macroscopic effects. Poor thermalization of the BFO source due to thermal contact resistance combined with radioactive heating. Depending on the decay scheme of the isotope used, source heating may be as high as 0.1 e/s, and if a good metallic contact to the source material is not achieved, relatively large temperature errors may result. This problem is avoidable if care is taken with sample mounting and if the source activity is carefully chosen with regard to the temperature desired. This limitation clearly becomes more serious as sample temperatures are lowered.

A second macroscopic effect is erroneous thermometry due to the effect of the applied field if an external ferromagnetic thermometer is used; this point is examined in detail below (Section 4.2).

(ii) Microscopic effects. Even if the host lattice is properly thermalized, the impurity nuclei may not be in equilibrium with it. One possible cause is a very long relaxation time T_1; this should not be a problem in metal samples, although it might become serious in insulators. It can in any case be detected by monitoring the time dependence of the observed effect for a period of hours or days.

A second cause of microscopic nonthermalization is the formation of "isolation clusters" in which the radioactive impurity atoms are concentrated in the form of a chemical compound (oxide, nitride, etc.). This can occur especially in thermally prepared samples if the impurities are not too soluble and/or are good "getters" for impurity gases present in the host lattice. Such clusters have been observed by metallographic means, e.g., in the purification of Cu by oxygen or chlorine annealing; the impurity atoms in the clusters may be effectively insulated from the host conduction electrons and will take on a higher spin temperature due to radioactive heating. Effects of this kind can be avoided by careful sample preparation, especially by the use of reduced starting materials and ultrahigh vacuum techniques or by in situ generation or implantation of the impurities (especially recoil implanation, which provides a more even distribution of impurities and fewer impurity–defect structures than separator implantation). Also, impurity–host combinations should be carefully chosen for solubility and chemical compatibility whenever possible—here the BFO method offers considerably more freedom than nuclear orientation in ferromagnets.

3.4. Anisotropy Measurement

In a BFO experiment, relatively small γ-ray anisotropies must be measured with good absolute accuracy. This can give rise to difficulties of several types, which may not be immediately recognizable:

(i) Electronic errors due to incorrect allowance for dead time in the counting system, pulse pileup, and time measurement errors. Such errors can be eliminated by testing the counting system with a pulser or single-line sources, but care must be taken in the design of the counting system.

(ii) Detector errors due to incorrect detector placement, erroneous solid angle corrections, detector drifts or stray field effects, and relative motion of the source and detectors. "Warm counts" should always be taken before and after each cold measurement without changing the magnetic field. Many commerical Ge(Li) detectors show a sensitivity to stray fields of order 0.5 T and may gradually change their characteristics in an applied field. A good method for detecting errors of types (i) and (ii) is the use of a single-line calibration source, preferably mounted in the cryostat near the BFO source and having a γ-ray energy below that of the lowest energy of interest in the BFO experiment.

(iii) Errors in calculating peak areas and in background corrections. Various authors have discussed methods for fitting γ-ray spectra and determining background corrections.[19] In our experience, a simple determination done by summing counts in the peak region with linear background interpolation is usually adequate for Ge(Li) spectra. Clearly the spectrum

must be recorded with sufficient resolution to permit accurate peak location and background estimation, and if the counting system is not gain-stabilized, provision for estimating the effect of fractional-channel drifts must be included in the analysis program. Krane *et al.*[20] have described a useful method of performing the background correction for a peak in a complex spectrum. A particularly pernicious source of error, which must be carefully avoided, is the presence of an unrecognized coincidence (sum) or impurity γ-ray peak under a peak of interest.

3.5. Resonance Experiments

The combination of brute-force orientation with NMR (BF/NMR) eliminates the errors due to thermometry and anisotropy measurement described above. Such an experiment allows the determination of the energy splitting Δ, and thus of g-factors, Knight shifts, and electric quadrupole splittings, with great accuracy. Using fast passage or pulse techniques, nuclear relaxation times may also be determined, although they may be nonresonantly measured by pulsed heating. BF/NMR may also be combined with a BFO measurement to determine the nuclear spin of the state on which resonance was performed, although it is not sensitive to intermediate spins or transition multipolarities. The resonance linewidths in cubic metal hosts should be similar to those observed in pure nonmagnetic metals, i.e., of order 10 kHz. There are basically two limitations to the performance of BF/NMR experiments:

(i) Achieving saturation of the resonance signal. In a BF/NMR experiment, one detects resonant destruction of nuclear alignment; a detectable signal is only obtained for large relative population changes, i.e., saturation. The saturation condition is given by[21]

$$\omega_1^2 T_1 T_2 \approx 1 \tag{5}$$

where $\omega_1 = g\mu_N H_1/\hbar$ is the precession frequency in the rf field H_1, and T_1 and T_2 are longitudinal and transverse nuclear relaxation times. For dilute systems usually $T_2 = T_1$ and Eq. (5) reduces to $(g\mu_N/\hbar)H_1 T_1 \approx 1$. For a given nucleus and relaxation time (typically of order 10 sec for the systems considered), a minimum value of H_1 is thus specified, equal to 0.02 mOe for $g = 1$ and $T_1 = 10$ sec. In practice, some inhomogeneous broadening will be present, so that not all the rf power can be supplied into a single homogeneous line and the effective H_1 may be reduced by a factor of ten or more. Applied H_1 values are limited to a few mOe by eddy current heating, although they might be considerably increased by using a dilution refrigerator with large metal–He contact area. Thus, achieving saturation should not be difficult as long as T_1 is greater than several hundred msec.

This situation is quantitatively similar to that of NMR on nuclei oriented in ferromagnets (NO/NMR); in the latter case, the inhomogeneous line broadening may be a factor of 100 or more larger than in BF/NMR, but the resulting loss in effective H_1 is compensated by ferromagnetic enhancement of the rf field. In many cases of NO/NMR, saturation has proved to be more difficult than indicated by Eq. (5),[22] and the same may be true in BF/NMR.

(ii) A second limitation in BF/NMR is the resonance linewidth. As indicated above, inhomogeneous line broadening makes saturation more difficult and may eventually make the signal unobservable. This could occur if the sample were not homogeneous, having a distribution of sites for the impurity atoms with different Knight shifts or quadrupole splittings; or if a large quadrupole splitting were present, especially for large nuclear spin; or if the external field were inhomogeneous or unstable. To ensure that field broadening of the resonance line is insignificant in BF/NMR, a magnet homogeneity of 10^{-5} or better over the sample is typically required, and a comparable field stability for the duration of the measurement (hours or days if signal averaging is used) is also needed. This may pose problems with the use of extremely high-field magnets.

4. APPARATUS REQUIREMENTS

In the present state of the art, application of BFO is essentially limited by available apparatus, so some discussion of the technical requirements of a BFO experiment and characteristics of a typical setup seems justified.

4.1. Cryostat

Figure 1 is a schematic of the apparatus used in Berlin for BFO and BF/NMR experiments. It is a conventional paramagnetic demagnetization apparatus using CMN as the primary cooling salt. The main salt pill contains 250 g of CMN powder in glycerin, making contact through 3600 cm^2 of silver foils to a heat link of 0.3-mm-diameter Cu wires potted in epoxy, having a cross section of 0.4 cm^2, length 35 cm, and attached with screw joints. The main feature of the apparatus is the large polarizing field of up to 7.5 T provided by a large-volume, high-homogeneity Nb–Ti solenoid. The stray field of this solenoid necessitates a long heat link (50 cm from center of salt pill to sample), which limits the minimum temperatures to 5–6 mK in the sample at low polarizing fields. At high polarizing fields, the sample temperature rises, partly due to stray field on the salt pills and partly to eddy current heating from vibrations of metal parts in the polarizing field. This is illustrated in Fig. 2. Figure 3 shows the maximum H/T values obtainable, which are near 450 T/K at $H = 6.5$ T.

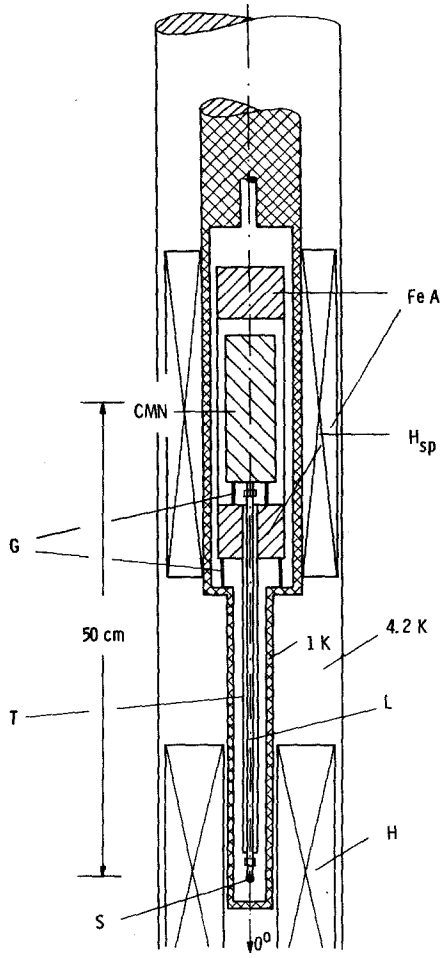

Fig. 1. Schematic of Berlin BFO apparatus. The outer vacuum jacket and liquid N_2 shield are not shown. Fe A, iron alum guard salts; CMN, main salt pill; G, graphite supports; T, thermal shield (coil foils); L, Cu wire thermal link with screw joints; S, sample, H_{sp}, demagnetization coil (4.0 T); H, polarizing coil (7.5 T). The rf leads and particle detector are omitted for clarity.

Experience with this apparatus has shown that it has several disadvantages for BFO experiments. The spatial extent of the stray field from the polarizing coil (which was designed with NMR experiments in mind) limits sample temperatures and causes difficulty with γ-ray detectors; the minimum source–detector distance is about 25 cm. Also, because of the thick coil windings, counting is only possible along the field axis. In general, for pure BFO experiments where field homogeneity is not critical, a small-volume split coil arrangement is probably superior, since it allows short detector–sample distances and counting from several directions, and its stray field is smaller, permitting lower sample temperatures, especially if

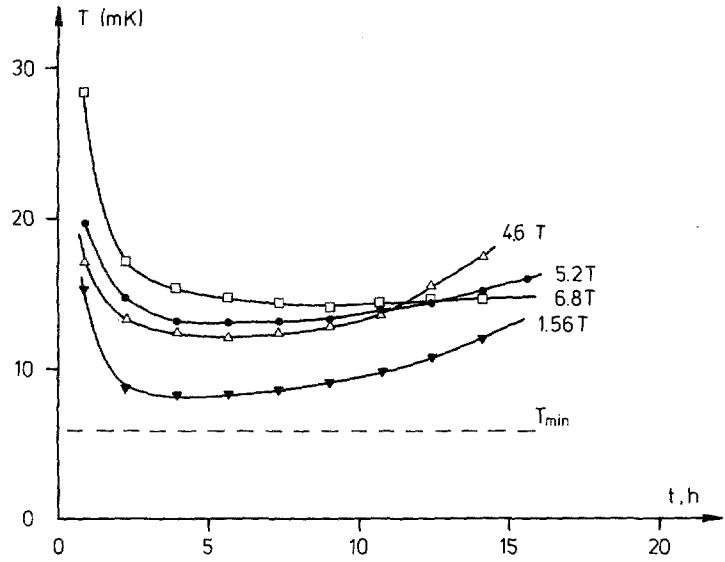

Fig. 2. Warming curves of the apparatus shown in Fig. 1; $t = 0$ corresponds to completion of demagnetization, and T_{min} is the temperature reached when $H < 0.5$ T.

some form of adiabatic demagnetization is used for cooling, and minimizing stray-field effects on the radiation detectors.

For BF/NMR experiments, however, homogeneity and field stability are essential, and some means for measuring and controlling the field during an experiment is required. For this application, the Berlin apparatus is also not ideal, although the magnet homogeneity is sufficiently good (better than 10^{-5} over 1.5 cm on the axis). Due to the presence of a large number of joints in the windings, the field decays at a rate of 22 ppm/h; also, precision field measurements can only be made by removing the low-temperature components and inserting a reentrant warm bore assembly to allow use of an H_2O–D_2O NMR probe. In general, it is probably impossible to optimize the characteristics of a single apparatus for both BFO and BF/NMR experiments, since the required properties are to some extent mutually exclusive.

One possibility for performing BF/NMR experiments at more modest H/T values is the detection of β particles. Since the β asymmetry increases as the polarization rather than the alignment, measurable effects can be obtained at smaller H/T, although quantitative measurements are made difficult by magnetic focusing and by scattering of the β particles. The feasibility of such measurements has been demonstrated by work on $^{60}CoAu$,[9] although good field stability is required.[23] In a BF/NMR experiment, where the asymmetry measurement only serves to indicate fulfillment

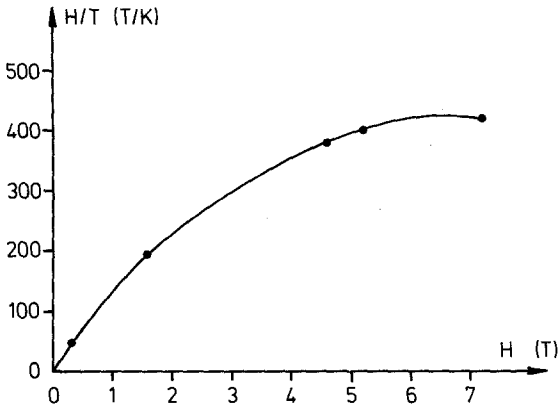

Fig. 3. H/T values obtained with the apparatus of Fig. 1, as a function of applied field H.

of the resonance condition and quantitative asymmetry measurements are thus unnecessary, β detection could greatly enlarge the application of the technique.

4.2. Thermometry

The question of accurate thermometry in large applied fields is central to BFO experiments. If some deviation in the temperature recorded by a nuclear thermometer were produced by the applied field (e.g., due to nonadditivity of the hyperfine field H_{hf} and H), then different nuclear thermometers with differing anisotropy curves and H_{hf} values should show disagreement at high applied fields. Such a comparison is shown in Fig. 4, where data from two commonly used thermometers (^{54}Mn*Ni* and ^{60}Co*Fe*) in fields up to 7 T are shown. At low H (below 2 T) and temperatures down to 8 mK, agreement is found to better than 0.5%. This is in contrast to a comparison of ^{54}Mn*Fe* and ^{60}Co*Fe* in the same source at low applied fields ($H < 0.3$ T) by Sites *et al.*,[24] who found ^{60}Co temperatures about 5% higher at 8 mK. At larger applied fields, a significant deviation appears in our experiments, amounting to $\Delta T/T = +3.8\%$ for ^{60}Co in the range $H = 4.6$–7.0 T between 12 and 20 mK (dashed line in Fig. 4). This deviation is not alarmingly large, although its origin is uncertain. If it were due to relaxation effects or to the greater radioactive heating in the ^{60}Co*Fe* foil, the deviation should be greater at the lowest temperatures, which is not the case. It is known[25] that Fe foils show much greater sensitivity to eddy-current heating at rf frequencies than do noble metals; in the present case, eddy current heating in the frequency range 10–1000 Hz is produced by mechanical vibrations of metal parts in the applied field, with the heating being

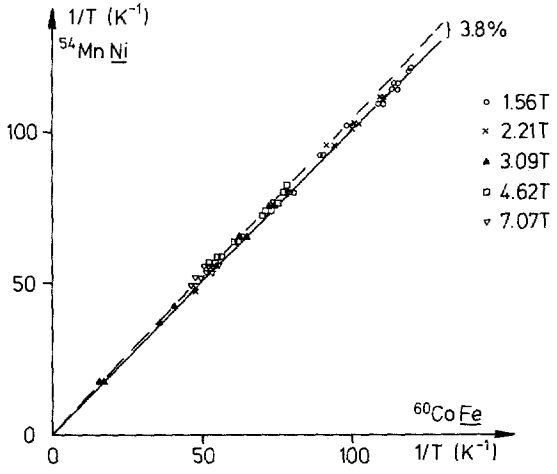

Fig. 4. Comparison of temperatures indicated by ^{60}Co*Fe* and ^{54}Mn*Ni* thermometers in high applied fields. The solid line indicates exact agreement; the dashed line is fitted to the high-field ($H > 4.5$ T) points. Double points are obtained from 1.17- and 1.33-MeV γ rays of ^{60}Co.

proportional to H^2 at a given vibration frequency. If the Fe foil is more strongly heated than Ni by these eddy currents, the observed deviation could be explained. Such an effect would presumably cause ferromagnetic nuclear thermometers to indicate incorrectly high temperatures compared to nonmagnetic BFO sources; this is, as will be seen below, not observed experimentally.

4.3. Tests of Data Accumulation System

In order to check our data accumulation and thermometry for systematic errors of the types mentioned in Sections 3.3 and 3.4, experiments were performed at high fields on source foils with well-known hyperfine interactions. Figure 5 illustrates such a study of ^{57}Co*Ni*, for which all parameters are well known from resonance experiments.[19,26] This is essentially a "reverse BFO" experiment, since H_{hf} has the value -12 T, so that at 6 T applied field, the net field acting on the nuclei is equal to the applied field but opposite in sign. The relatively large statistical errors on individual points are due to the small anisotropies observed; however, no systematic effects in H or H/T are seen. The weighted average for H_{hf} is in excellent agreement with the NMR value (shown as a shaded band in Fig. 5). A similar experiment on ^{58}Co*Fe* also showed no systematic deviations and an average H_{hf} in agreement with the NMR value.

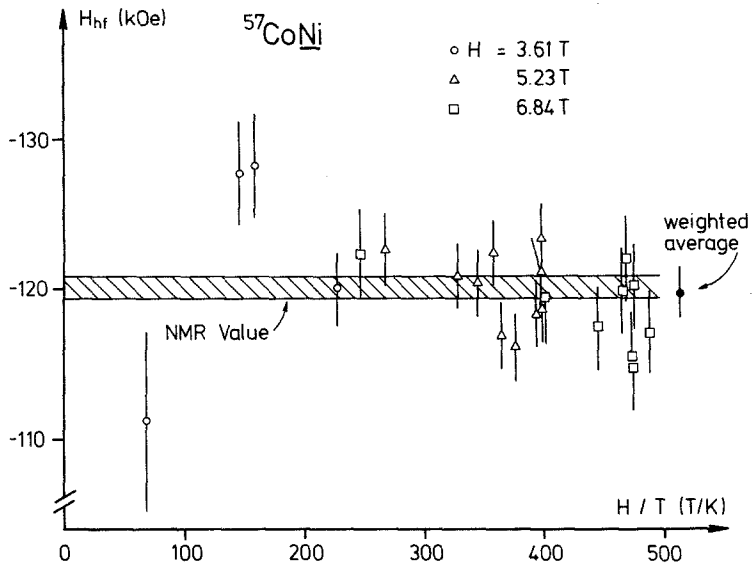

Fig. 5. Hyperfine field H_{hf} at ^{57}Co*Ni* measured at large H/T values to check for systematic errors, shown for three applied fields as function of H/T. The shaded region is the NMR result; the solid point with error bars is the weighted average of nuclear orientation points.

For the peak analysis of γ spectra, well resolved peaks and background are important. For studying γ peaks that are widely separated in an otherwise uninteresting spectrum, the arrangement shown in Fig. 6 is useful. The spectral regions of interest are selected in single-channel analyzers and gated into biased amplifiers, where they are expanded and shifted to fill one whole memory block (512 or 1024 channels) of a multichannel analyzer. After remixing, the pulses enter the analyzer, giving a spectrum which allows simple and accurate peak-area determination. The example shown is a γ spectrum of ^{57}Co and ^{60}Co. Care must be taken, however, that additional dead-time or pileup problems are not introduced in such a setup; this is particularly serious if a strong additional peak is present in the spectrum or at high overall count rates.

5. EXPERIMENTAL RESULTS

5.1. Survey

The results of BFO experiments using γ-ray anisotropies which have been reported to July 1976 are summarized in Table I. In most cases, nuclear parameters were known from NMR experiments or could be theoretically

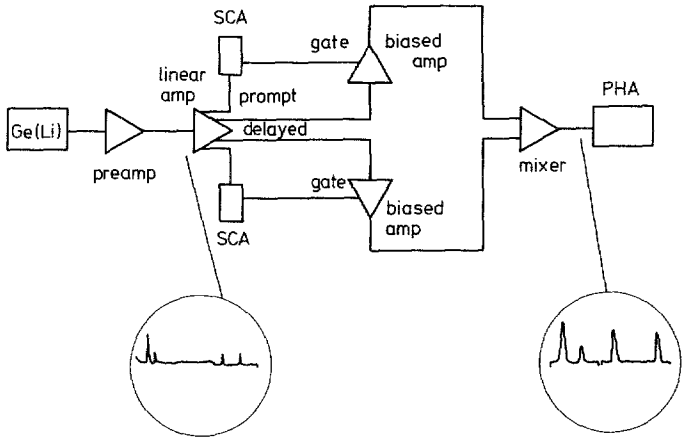

Fig. 6. Schematic of "spectrum-stretcher" setup used to study widely separated γ-ray peaks. SCA, single-channel analyzer; PHA, pulse height analyzer; typical spectra are shown for $^{57}Co + {}^{60}Co$.

estimated with confidence, so that the theoretically expected anisotropy could be calculated. In many cases, an attenuation of the experimental results was observed. This is expressed as an attenuation factor α in the second column of the table; α is defined as the factor which, when multiplied by the known β value and used in Eqs. (1) and (2), yields a satisfactory fit to the data over the observed range of H/T. This treatment is thus equivalent to assuming a uniform attenuation of H or increase of T in the sample (e.g., a large, negative Knight shift or a macroscopic temperature error), or an "effective g-factor" reduced from the true value.[31] Such a hypothesis is of course not unique—one could also, for example, assume that some fraction f of the sample nuclei were not oriented or incompletely oriented (e.g., those in isolation clusters), so that a weighted average of appropriate anisotropy functions [Eq. (1)] should be used to fit the data [if only the B_2 term in Eq. (1) is important, this assumption is equivalent to including an attenuation coefficient G_2 in the anisotropy function; see table footnotes]. A third possible hypothesis is that the local orientation axis is not parallel to H throughout the sample—this would be the case in the presence of a randomly oriented, strong electric quadrupole perturbation or of local moments acted on by a random molecular field. The anisotropy function would then need to be suitably averaged over angles θ. This hypothesis is, however, usually unsuited to the analysis of BFO results, where the sources are chosen to have only small hyperfine interactions.

Choosing between the first two hypotheses is, in fact, surprisingly difficult in the H/T range of interest. This is shown in Fig. 7, in which curves

TABLE I

BFO Experiments

Case	Attenuation factor	Group	Remarks
^{60}Co*Au*	1.00(8)	Minnesota, 1970[27]	$H_0 = 2.5$–4.1 T; $K = +29.2\%$[47] (NMR)
^{60}Co*Au*	0.998(14)	Berlin, 1973[9,a]	$H_0 = 7.2$ T
^{93}Mo^m*Nb*	0.82(5)	Berkeley, 1972[28a]	$H_0 = 4.5$ T, moment corrected.[b] Cu deposition mounting, in situ activation
^{93}Mo^m*Nb*	~0.7	Melbourne, 1973[29]	As above
^{110}Ag^m*Ag*	1.027(11)	Berlin, 1973–6[c]	Corrected for $K = +0.52\%$; in situ activation
^{110}Ag^m*Cu*	~1.0	Oxford, 1974[30]	
^{111}In*Cu*	0.82(4)	Oxford, 1974[31]	BF/NMR search
^{114}In^m*In* s.c.	0.67(4)[d] [0.87(5)]	Berlin, 1974[c]	Cu-plate mounting; in situ activation; possible electric quadrupole interaction
^{95}Nb*Pt*	1.029(16)	Leyden, 1975[13]	K uncertain (<0?); thermometry
^{95}Nb*Cu*	0.35(2)	Berlin, 1975[32]	Strong sample dependence
^{95}Nb*Nb*	0.858(24)	Berlin, 1975[32]	
^{95}Nb*Ta*	1.004(2),[e]	Berlin, 1975[32,c]	High temperature, UHV diffusion; BF/NMR sources
^{87}Y^m*Au*	0.93(9)[g]	Lyon, 1975–6[33]	Implanted source; 100% attenuation on annealing or melting
^{87}Y^m*Al*	1.0[h]	Lyon, 1976[33]	Unannealed; 50% attenuation on melting
^{87}Y^m*YAl*$_2$	0.47[g]	Lyon, 1976[33]	Stoichiometric intermetallic (possible electric quadrupole interaction)
^{57,58,60}Co*Mo*	0.980(12)[i] [1.001(19)]	Berlin, 1976[c]	$K = -8.0\%$ (NMR[35]); field dependence

[a] With J. Flouquet.

[b] Samples mounted by vacuum deposition of Cu followed by soldering: ^{93}Mo^m moment corrected to new value reported by Eska *et al.*[28b]

[c] This work.

[d] Sample mounted by overplating with Cu; the attenuation in brackets is obtained by allowing for an axial, positive electric quadrupole frequency $eqQ/h = 45.2$ MHz, parallel to H.

[e] Sample I: evaporated.

[f] Sample II: plated.

[g] Attenuation expressed as a perturbation factor G_2 which multiplies B_2 in Eq. (1); higher terms are neglected.

[h] Taken to be unattenuated, corresponding to a nuclear moment of $5.90(14)\mu_N$ for ^{87}Y^m($9/2^+$).[33]

[i] Weighted average for all applied fields (Fig. 12); the value in brackets is for high applied fields (6.5, 7.0 T) only.

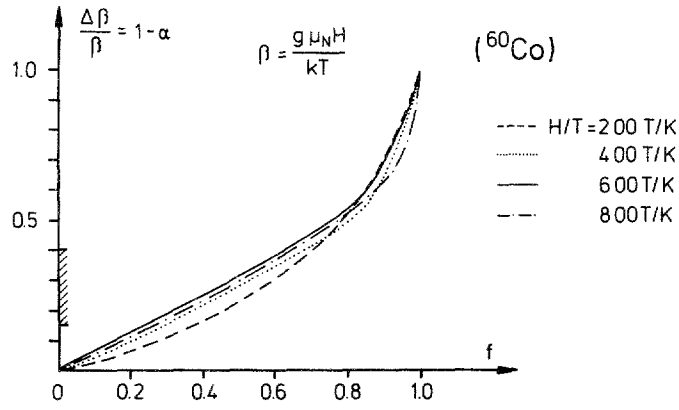

Fig. 7. Curves showing the values of the fractional reduction of energy ratio β (related to attenuation parameter α as indicated) that give the same anisotropy as a fraction f of nonoriented nuclei, calculated using ^{60}Co decay scheme with H/T as parameter. Shaded region on the ordinate indicates the range of α values seen in some BFO experiments (Table I).

are drawn connecting values of fractional β attenuation ($\Delta\beta/\beta = 1-\alpha$, ordinate) that, for a given H/T value, yield the same anisotropy as a fraction f of unoriented nuclei (abscissa). These curves, calculated using the anisotropy function for ^{60}Co, are nearly the same over a large range of H/T; for large H/T and attenuations of less than 50% they are in fact identical. This is because the anisotropy function is nearly linear in β in the middle region of H/T values, so α and f simply scale together. In the region of small H/T values, where the curvature of the anisotropy function is greater, the anisotropy itself is too small to allow accurate comparison. Only in the saturation region of large H/T values—currently inaccessible to BFO experiments—can one sensitively select the correct fit hypothesis by comparing anisotropy data as a function of H/T with curves calculated on the above models. The attenuation parameters shown in Table I are thus a reasonable indicator of an observed deviation of the data from expected values, regardless of the precise mechanism which produces the deviations.

Figures 8–10 show the anisotropy data on which some of the entries in Table I are based. In most cases, H/T values from 100 to 500 T/K were available, and although the individual points show large errors and the observed effects are small, accurate fits to the anisotropy can be achieved by taking many data points.

Of the 14 cases cited in Table I, about half show agreement within two standard deviations with theoretical expectations. The others show an attenuation in the range 15–50%. In two cases (^{93}Mo^{m}*Nb* and ^{114}In^{m}*In*) in

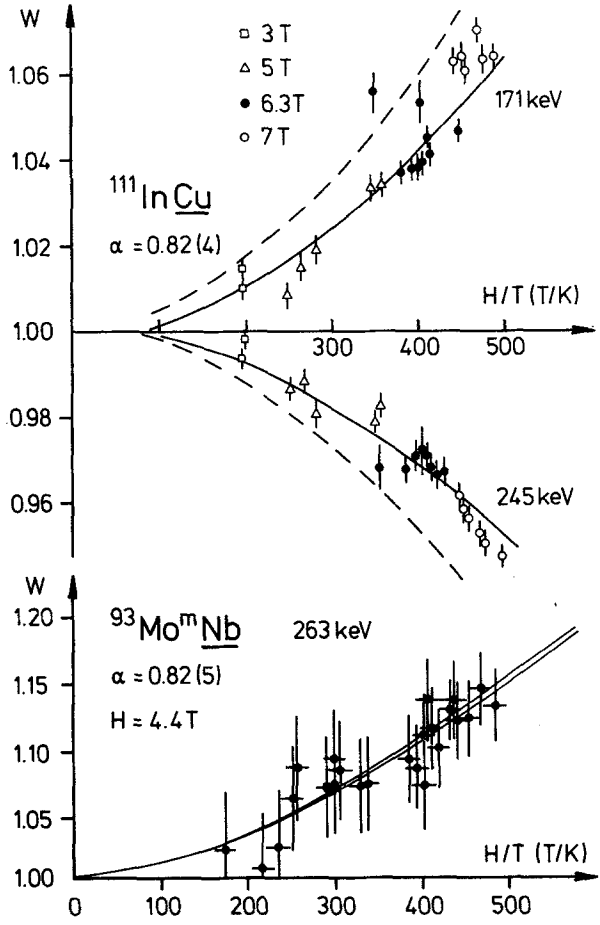

Fig. 8. BFO data for two cases: upper curves, ^{111}In*Cu* (Ref. 31); dashed curves are expected anisotropy W at 0°; solid curves are fit to data points giving α value shown. Lower curve: ^{93}Mo^{m}*Nb* (Ref. 28a); the two solid lines show error limits to fit, giving $\mu_{(21/2)} = (8.1 \pm 0.35)\mu_N$. The most recent NMR result is $9.89 \pm 0.18\mu_N$ (see Ref. 28b), giving the value of α indicated.

which the impurity nuclei were generated in situ and the samples were not annealed, the deviations were probably due to macroscopic temperature errors (sample mounting was in both cases difficult) or to incorrect anisotropy determination. However, a hyperfine perturbation due to impurity-associated radiation damage cannot be conclusively ruled out without further experiments. In the In single-crystal experiment, part of the attenuation is probably due to the electric quadrupole interaction, but this cannot explain the whole observed deviation (see footnotes, Table I).

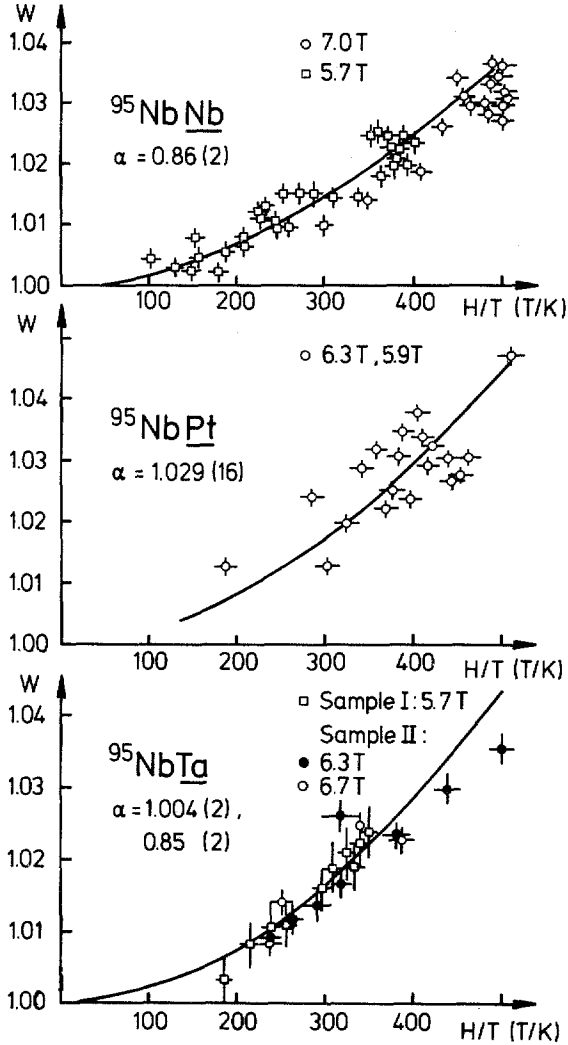

Fig. 9. BFO results on ^{95}Nb in various host lattices. Upper curve: ^{95}Nb*Nb* (Ref. 32); middle curve: ^{95}Nb*Pt* (Ref. 13); lower curve: ^{95}Nb*Ta* (this work and Ref. 32). All α values are uncorrected for Knight shifts.

In the remaining cases, metallurgical difficulties—formation of isolation clusters—are most likely responsible for the deviations. This is supported in several cases by thermal treatment of the samples, which produced a drastic change in the observed effects and sometimes gave total attenua-

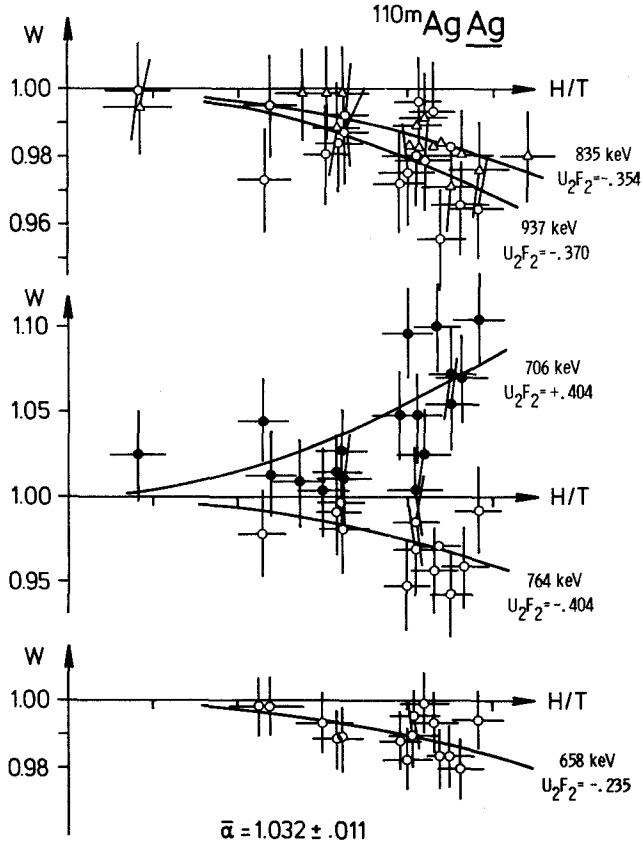

Fig. 10. BFO results for $W(0)$ vs. H/T on $^{110}Ag^{m}Ag$ using $^{54}MnNi$ thermometer. Several different γ rays were observed; $\bar{a}$ is a weighted average for the attenuation parameter without Knight shift correction (this work).

tion. Some of the impurities studied in these cases (Nb, Y) are good "getters" and also relatively insoluble in the hosts used, this making the formation of isolation clusters likely. The one exception is $^{111}InCu$,[31] where the solubility is high[34] and In has relatively tractible chemical properties, although it does form a nitride and oxides stable to relatively high temperatures. With Cu sources, thermal contact problems seem unlikely, and three samples gave consistent results. A mixed γ-transition renders the analysis of one γ peak uncertain, but both peaks gave the same deviation (Fig. 8). The attenuation in this case thus remains unexplained.

5.2. Co*Mo* Results

The case of Co*Mo* will be treated in more detail. This might be termed a "super-BFO" experiment since a large, negative Knight shift attenuates the applied field. This system was studied by Narath *et al.*[35] using NMR, and a concentration-dependent Knight shift of about −8% was observed (Fig. 11). A later study also showed the existence of an unshifted Co site due to formation of the intermetallic compound Mo_6Co_7.

Our samples contained very low added Co concentrations (Table II). One of them was also used in a Mössbauer study of Fe*Mo*,[36] and showed relatively narrow Mössbauer lines in zero field even at very low temperatures, indicating the absence of magnetic clustering. In all, seven BFO measurements were performed using the various Co*Mo* samples in combination with ^{54}Mn*Ni*, ^{60}Co*Fe*, and ^{58}Co*Fe* nuclear thermometers at temperatures of 8–20 mK and fields of 1.5–7 T. Figure 12 shows the results, given as Knight shift observed vs. applied field. The shaded region shows a weighted average of all points, and the short, cross-hatched bar shows the NMR results extrapolated to zero Co concentration. A field dependence is seen to be present; the same dependence was observed with each sample/thermometer combination. No dependence of the resonance shift on applied field was found in the NMR experiments. Even if the deviation of the low-field points is discounted because of their large statistical errors, the points at $H = 3.5$ and 5.0 T must be seen to be significantly shifted. The source of this field dependence is unclear; as pointed out in Section 4.3, no such field-dependent effects were seen with ferromagnetic-host alloys. The

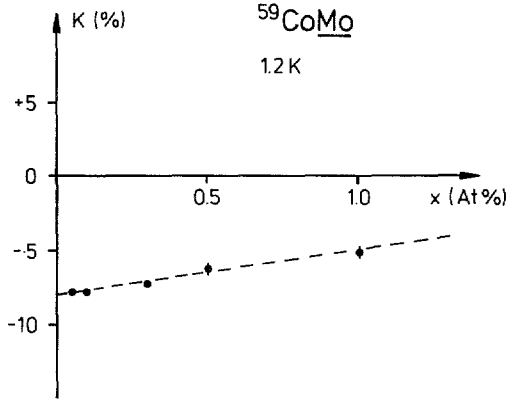

Fig. 11. Knight shifts of Co in Mo observed by Narath *et al.*[35] with NMR as a function of Co concentration x (at %) at a temperature of 1.2 K.

TABLE II

Sample Preparation, Co*Mo*[a]

Alloy	Added Co, ppm	Preparation method	Final form	Radioactivity, μCi
^{60}Co*Mo*	5	Arc melting, Ar atmosphere	2-mm sphere	5
^{57}Co*Mo*[b]	50	Diffusion 1800°C, H_2	150-μm foil	150
^{58}Co*Mo*	<1	Diffusion, 1650°C, H_2	120-μm foil	8

[a]Starting materials: Carrier-free radioisotopes, 99.95% Mo (Metals Research, VP Grade). Resistivity ratio: 50.
[b]Sample I from Pérez-Ramirez *et al.*[36]

reproducibility of the field dependence among samples prepared in different ways with different impurity isotopes suggests that the effect is not due simply to bad metallurgy. The BFO technique is of course integral and sums the contributions from all impurity nuclei, unlike NMR, which is unaffected by impurities, e.g., in magnetic sites; this could account for a uniform deviation of the BFO result from the NMR value, although the strong minimum as a function of H seen in Fig. 12 is difficult to explain. The high-field points at $H = 6.6$ and 7.0 T give excellent agreement with the NMR value.

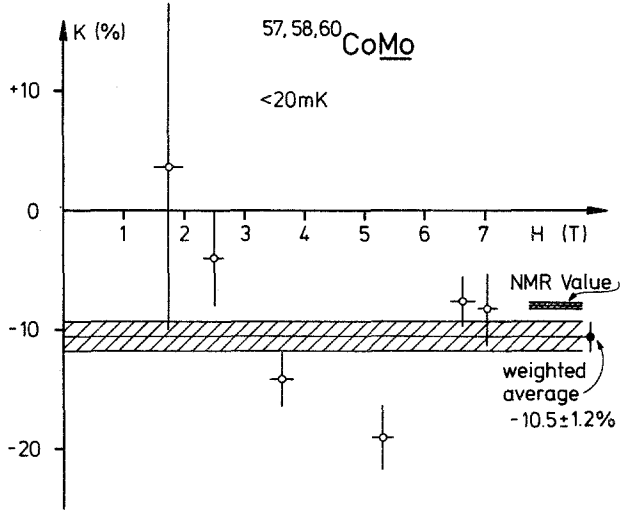

Fig. 12. Knight shifts from a BFO experiment on Co*Mo* plotted vs. applied field H. The points are averaged from seven runs with various source–thermometer combinations; errors indicate scatter. The broad, shaded band is the weighted average of all points as indicated; the short, cross-hatched band is the (field-independent) NMR value extrapolated to zero Co concentration (see Fig. 11).

In summary, while the practicability of BFO has been demonstrated, some pitfalls are present, and in particular attention must be paid to metallurgical problems in sample preparation; these seem to play a greater role than in nuclear orientation in ferromagnetic hosts, at least in the host–impurity combinations so far examined. It has been suggested by Berkes[37] that some of these difficulties may be avoided by the use of intermetallic compounds as hosts, in which the impurities occupy well-defined stoichiometric lattice sites. This may be of assistance in some cases, although preparation of the intermetallics often provides its own metallurgical difficulties and they are frequently brittle and difficult to handle.

6. NUCLEAR RESONANCE ON BRUTE-FORCE-ORIENTED NUCLEI

The advantages of nuclear resonance on nuclei oriented by BFO, or BF/NMR, have been discussed above. This technique should, with currently available apparatus, be applicable to many systems and should complement the now widespread NO/NMR technique.

A BF/NMR experiment was carried out at Oxford in 1974 on the ^{111}In*Cu* system.[38] The resonance lines were unexpectedly wide and barely observable outside counting statistics, and the experiments were not pursued.

Experiments on BF/NMR of ^{95}Nb were also begun in our laboratory about this time. The g-factor of the $35d$, $I = 9/2$ state was determined by NO/NMR in Fe host,[39] and the decay scheme is satisfyingly simple; there is, however, some uncertainty in the mixing ratio of the 765-keV γ transition.[40] This isotope in Pt host was studied as a BFO thermometer by Kontor and Hunik.[13] The metallurgical difficulties in this host seem to be minimal, and in fact a small enhancement of the BFO effect would appear to be present, expecially if the (probably negative) Knight shift is taken into account, although this enhancement is too small to be considered significant.

6.1. Source Preparation and Resonance Search

In initial experiments on ^{95}Nb*Cu*, a large attenuation of the BFO effect was found after H_2 reduction and diffusion (Table I); also, various samples gave unreproducible results. Samples of ^{95}Nb*Nb* were then prepared which also showed about 15% attenuation, possibly due to incomplete reduction of the Nb during diffusion, leading to formation of isolation clusters, or to poor thermal contact to the sample, although the latter seems unlikely. Attempts to observe the magnetic resonance of ^{95}Nb in these samples were unsuccessful. One possible explanation is that the g-factors of the ^{95}Nb

impurities and the ^{93}Nb host nuclei are nearly identical, so that spin–spin relaxation of the impurities to the host nuclei can occur, making T_2 short and fulfillment of the sauration condition, Eq. (5), impossible. (This argument is, however, contradicted by the final results of BF/NMR on ^{95}Nb.)

Finally, ^{95}Nb*Ta* sources were prepared. Because of the high melting point of Ta, diffusion of ^{95}Nb can be carried out at high temperatures ($T \geq 2200$ K) in ultra high vacuum ($p < 10^{-9}$ Torr). The effect of small impurity concentrations in Ta has been studied extensively by Mössbauer effect.[41] Source I, prepared by diffusing about 10 μCi of ^{95}Nb at 2150 K and 4×10^{-9} Torr after deposition from a methanolic solution onto the 6-μm-thick Ta foil, gave nearly perfect agreement with the expected anisotropy. A resonance line was observed at 63.5 MHz in a field of 6.22 T and at 65.9 MHz in 6.46 T. The lines were broad (70–90 kHz) and their areas implied 25–50% destruction of the γ-ray anisotropy. Preliminary results of this experiment were given at the Leuven Meeting on Hyperfine Interactions.[32]

A second ^{95}Nb*Ta* sample was prepared in a way similar to the first except that the Nb activity was electroplated onto a 5-mm circular spot on the Ta foil and diffused for a somewhat longer time. The Nb concentration in both samples was less than 1 ppm. Sample II showed some attenuation of the BFO (Table I). The γ-ray anisotropy observed with a NaI(Tl) detector in two energy regions is shown in Fig. 13, where the effect of rf heating of a 60-MHz high-frequency field of various strengths H_1 is also shown. Some resonance lines obtained at $H = 6.335$ T and $H_1 = 3$–4 mOe are given in Fig. 14, along with a control sweep made with the sample at 4.2 K. These lines were obtained after signal averaging for 10–12 h. They show smaller resonance destruction than with sample I, ranging from 7.5% to 24%, but have linewidths of 20–25 kHz. The remaining linewidth may be partly due to drift of the magnetic field H during each experiment, which was equivalent to a frequency drift of nearly 15 kHz. For this reason and because the field could not be exactly reproduced in successive runs, it was difficult to sum many runs to improve statistics; this emphasizes the importance of a stable, NMR-controlled polarizing magnet.

6.2. Analysis of NMR Results

In a BF/NMR experiment, the impurity atoms should carry no moments and no hyperfine field should be present; a plot of resonance frequency vs. field should then be a straight line through the origin whose slope is given by

$$\frac{d\nu}{dH} = \frac{g\mu_N}{h}(1+K) \tag{6}$$

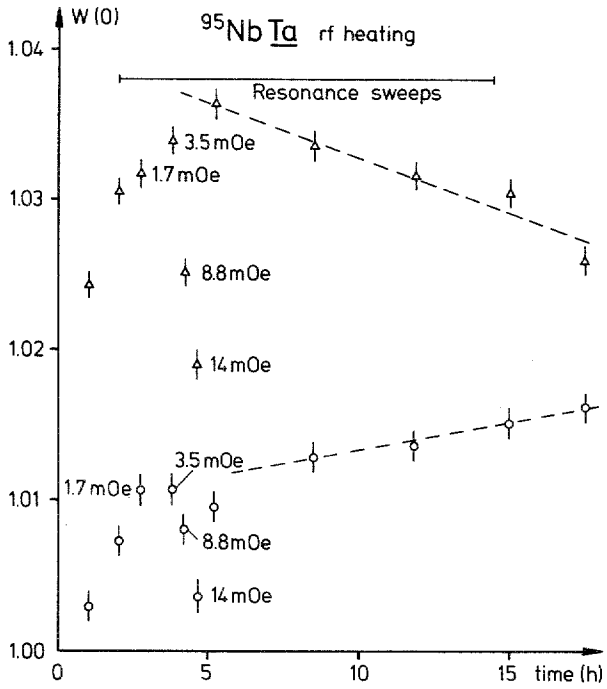

Fig. 13. Observed γ-ray anisotropy in the 765-keV γ-ray peak from ^{95}Nb*Ta* (triangles) and in the region 50–150 keV (circles) using a Na(Tl)I detector. In the low-energy region, counts from the ^{57}Co*Fe* thermometer source are also present. Demagnetization was completed at $t = 0$; the effect of rf heating by a 60-MHz signal with H_1 as shown was studied. Later resonance sweeps were carried out during the time period indicated by the horizontal line.

where g is the nuclear g-factor and K the Knight shift. A plot of the BF/NMR points from ^{95}Nb*Ta* is given in Fig. 15. If all points are simply fitted to a straight line, the dashed curve results, which, however, does not extrapolate to the origin but rather to 7.2 MHz at $H = 0$. The slope of the line is also rather inaccurately determined, since only a small range of H values is covered in the fit. If the line is forced to go through the origin, the solid curve in Fig. 15 results. Its slope is much more accurately determined, being equal to 0.10227(17) MHz/T. The errors include the shaded region shown in the figure and a recent magnet recalibration was taken into account.

This value of the slope can be compared with the g-factor obtained from NO/NMR. This is done in Table III. The zero-field resonance frequency from a spin-echo experiment on stable ^{93}Nb in Fe (Ref. 42) can be

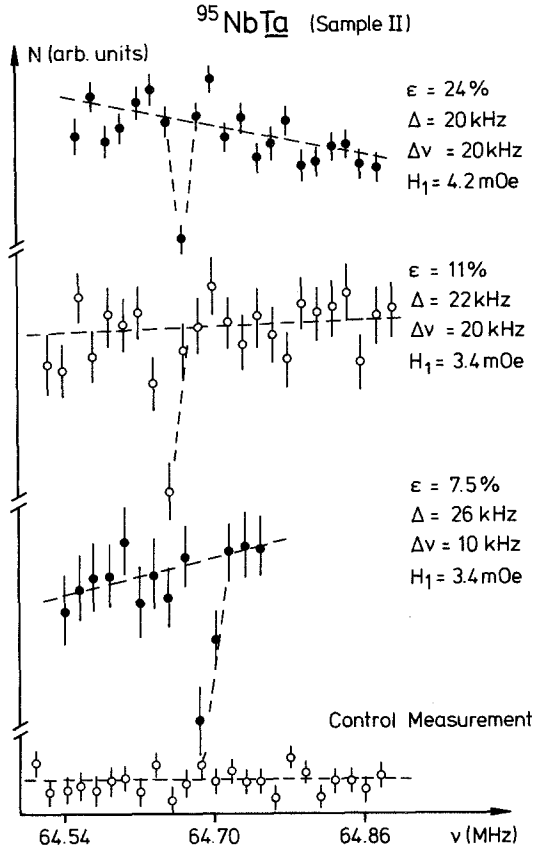

Fig. 14. Some BF/NMR lines obtained with ^{95}Nb*Ta* sample II at $H = 6.335$ T. The parameter ε is the percent of resonant anisotropy destruction (integrated over the line, corrected for modulation); Δ is the linewidth; $\Delta\nu$ is the fm bandwidth at 100 Hz modulation frequency (triangle wave); and H_1 is the rf field strength of one rotating component. The control measurement was performed with H and H_1 on but with the source at 4.2 K.

combined with that of our NO/NMR measurement on ^{95}Nb in Fe (Ref. 39) and with the known g-factor of ^{93}Nb (Ref. 43) to yield the g-factor of ^{95}Nb, multiplied by a correction factor $(1+{}^{93}\Delta^{95})$ for a possible hyperfine anomaly. The latter should be small (<0.2%) since the two isotopes have very similar nuclear structure. This value (line 4, Table III) can be compared with that from the slope of the line in Fig. 15 (line 5). The Knight shift K of Nb*Ta* should have a value near +1.0%.[44] The result is shown in line 6: The

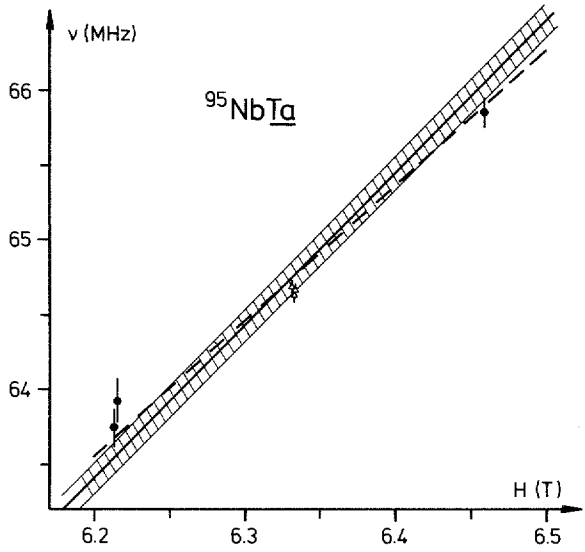

Fig. 15. BF/NMR resonance frequencies for ^{95}Nb*Ta* (circles, sample I; triangles, sample II) plotted against H. The dashed line is a linear least squares fit and does not go through the origin; the solid line with errors shown by shading is best fit when forced to go through the origin.

g-factor from the BF/NMR determination is $1.3 \pm 0.3\%$ smaller than that from the ferromagnetic-host measurements, if hyperfine anomaly and Knight shift are neglected. If the probable value of K is included, the discrepancy increases to $2.3 \pm 0.5\%$.

Although the data points in Fig. 15 show considerable scatter, possibly

TABLE III

Evaluation of ^{95}Nb g-Factor[a]

	Quantity	Value	Method	Reference
1	$g(^{93}\text{Nb})$	1.36515(7)	NMR(Nb_2O_5)	Sheriff and Williams[43]
2	$\nu_0(^{93}\text{Nb}Fe)$	276.5(2) MHz	Spin echo (1% alloy)	Koi *et al.*[42]
3	$\nu_0(^{95}\text{Nb}Fe)$	275.2(2) MHz	NO/NMR (0.2-ppm alloy)	Kopp and Brewer[39]
4	$g(^{95}\text{Nb})(1+{}^{93}\Delta^{95})$	1.3587(20)	Combining lines 1–3	—
5	$g(^{95}\text{Nb})(1+K)$	1.3417(22)	BF/NMR(^{95}Nb*Ta*)	This work
6	Δg	−1.3(3)%	Combining lines 4 and 5 with Δ, $K=0$	—
7	Δg(corr)	−2.3(5)%	Combining lines 4 and 5 with $\Delta=0$, $K=+1.0(2)\%$[44]	—

[a]Data for comparison of $g(^{95}\text{Nb}, 9/2+)$ by various methods. Quoted ^{93}Nb g-factor is uncorrected for atomic diamagnetism.

due in part to change in field calibration during the course of the measurements, this is included in the quoted errors and cannot explain the observed shift. The only steps in Table III where such a shift is likely to arise are lines 2 and 3, the resonance experiments in Fe host. The spin-echo measurement[42] was done with Fe powder, containing nominally 1% ^{93}Nb, in zero field; the resonance lines were broad (4 MHz) and the quoted frequency was from a fit to the line centroid. The signal was almost certainly due to nuclei in domain walls, and most of the Nb nuclei were probably in clusters or grain boundaries or in intermetallic compounds since the solid solubility of Nb in Fe is well below 1%.[34]

The NO/NMR experiment, on the other hand, was done with magnetically saturated Fe foils with less than 1 ppm Nb concentration and ν_0 was obtained by extrapolation to zero applied field. The lines were relatively narrow (0.5 MHz) but showed asymmetry and in some cases satellites, and sample-dependent shifts of resonance frequency totaling 0.75 MHz (~0.3%) were observed.[39] Attempts to detect the resonance in Fe single crystals were unsuccessful. Thus in both cases, a dependence of the resonance frequency on the local environment of the Nb atoms was seen, and this environment was almost certainly different in the two experiments. Direct comparison of hyperfine fields (or resonance frequencies) to within quoted fit errors from zero-field spin-echo measurements on concentrated ferromagnetic alloys with results on dilute, magnetically saturated NO/NMR samples may be a somewhat dubious procedure, especially for "difficult" impurities like Nb. Large resonance shifts between domain walls and wall edges or domain interiors have been observed for anisotropic lattices such as hcp Co,[45] amounting to effects of several percent. Such large shifts would be unexpected in the cubic Fe lattice, but since the exact magnetic locations of impurities in the two types of experiment may be different, a total shift of 2% seems possible. Under this interpretation, the correct ^{95}Nb(9/2+) g-factor would be given by the BF/NMR result, corrected for Knight shift, which is equal to 1.3284(26).* The corresponding moment is $6.004(12)\mu_N$, about 2.8% smaller than the ^{93}Nb(9/2+) moment. This difference, while relatively large for two such similar nuclei, is not outside the variation observed for the $\pi(9/2+)$ state.[46,39] The correct hyperfine field for dilute Nb in Fe domains would then be 27.17(8) T.

7. CONCLUSIONS

A number of experiments in various laboratories have demonstrated the feasibility of brute-force orientation for g-factor measurements, nuclear thermometry, and even Knight shift measurements on extremely dilute

* Uncorrected for atomic diamagnetism.

alloys. These initial experiments have pointed up some difficulties, most of which can be understood in the light of the limitations described in Section 3. In particular, sample preparation appears to present more problems than might have been expected and considerable attention must be paid to avoiding metallurgical difficulties when planning a BFO experiment. Soldering with In (using ultrasonic tinning when necessary) seems to give reliable thermal contact in most cases and an internal BFO thermometer should be used if possible.

Nuclear magnetic resonance on nuclei oriented by the BFO method has also been demonstrated. The observed resonance lines were somewhat broader than expected and rather small resonant anisotropy destruction (<50%) was obtained. The g-factor found for ^{95}Nb shows a shift relative to the value deduced from spin-echo and NO/NMR experiments in Fe host, which may imply that the effective hyperfine fields observed in the latter two types of measurement are not always identical, particularly with chemically active, relatively insoluble impurity atoms. The BF/NMR experiments emphasize the need for a homogeneous, stable, continuously measurable static field and for signal averaging techniques.

As attainable H/T values increase, these techniques will undoubtedly find considerable application, especially in cases where orientation in ferromagnetic hosts is difficult or impossible. Several groups are now planning experiments or setting up apparatus for BFO and BF/NMR. The universal applicability of the brute-force techniques gives them a powerful advantage over other methods of nuclear orientation.

ACKNOWLEDGMENTS

Thanks are due to Profs. I. Berkes and J. A. Barclay and to Drs. N. J. Stone, G. Eska, and J. A. Kontor, who communicated unpublished results. The assistance of Prof. E. Klein, G. Muschert, M. Kopp, and J. Boysen with apparatus and experimental details is acknowledged.

REFERENCES

1. C. J. Gorter, *Phys. Z.* **35**, 923 (1934).
2. N. Kurti and F. E. Simon, *Proc. Roy. Soc. A* **149**, 512 (1935).
3. R. J. Blin-Stoyle and M. A. Grace, in *Handbuch der Physik* **42**, (1957), p. 555.
4. M. I. Aalto, H. K. Collan, R. G. Gylling, and K. O. Nores, *Rev. Sci. Instr.* **44**, 1075 (1973).
5. A. I. Ahonen, P. M. Berglund, M. T. Haikala, M. T. Krusius, O. V. Lounasmaa, and M. A. Paalanen, *Cryogenics* **16**, 521 (1976).
6. K. Andres and J. H. Wernick, *Rev. Sci. Instr.* **44**, 1186 (1973); J. H. Bishop, E. C. Hirschkoff, and J. C. Wheatley, *J. Low Temp. Phys.* **5**, 607 (1971).
7. J. W. T. Dabbs, L. D. Roberts, and S. Bernstein, *Phys. Rev.* **98**, 1512 (1955); A. Stolovy, *Phys. Rev.* **118**, 211 (1960); H. Marshak, *Bull. Am. Phys. Soc.* **117**, 305 (1962).

8. H. Marshak, private communication (1976).
9. J. Boysen, W. D. Brewer, and J. Flouquet, *Solid State Commun.* **12**, 1095 (1973).
10. K. S. Krane, *Nuclear Data Tables* **11**, 407 (1973); S. R. de Groot, H. A. Tolhoek, and W. Huiskamp, in *Alpha-, Beta-, and Gamma-Ray Spectroscopy*, K. Siegbahn, ed. (North-Holland, Amsterdam, 1968), Vol. 2, p. 1199.
11. R. M. Steffen, Los Alamos Scientific Laboratory Report No. LA 4565-MS (1971).
12. N. J. Stone, *Hyperfine Interactions* **2**, 45 (1976).
13. J. A. Kontor and R. Hunik, in *Proc. 14th Int. Conf. Low Temp. Phys.*, M. Krusius and M. Vuorio, eds. (North-Holland, Amsterdam, 1975), Vol. 4, p. 52; J. A. Kontor, Ph.D. Thesis, Leyden, unpublished (1976).
14. E. Matthias, B. Olsen, D. A. Shirley, J. E. Templeton, and R. M. Steffen, *Phys. Rev. A* **4**, 1626 (1971).
15. G. Frossati and D. Thoulouze, in *Proc. ICEC 5, Kyoto, 1974*, p. 229.
16. E. N. Smith, H. M. Bozler, W. S. Truscott, R. C. Richardson, and D. M. Lee, in *Proc. 14th Int. Conf. Low Temp. Phys.*, M. Krusius and M. Vuorio, eds. (North-Holland, Amsterdam, 1975), Vol. 4, p. 9.
17. K. Andres, E. Hagn, and E. Smolic, *J. Appl. Phys.* **46**, 2752 (1975).
18. R. G. Gylling, in *Low Temperature Physics—LT 13* (Plenum Press, New York, 1974), Vol. 4, p. 487.
19. H. Marshak and R. J. Soulen, Jr., in *Low Temperature Physics—LT 13*, Vol. 4, p. 498; J. J. Huntzicker, Ph.D. Thesis, Berkeley, unpublished (1968); E. J. Cohen, A. J. Becker, N. K. Cheung, and H. E. Henrikson, *Hyperfine Interactions* **1**, 193 (1975).
20. K. S. Krane, C. E. Olsen, J. R. Sites, and W. A. Steyert, *Phys. Rev. C* **4**, 1906 (1971).
21. A. Abragam, *Principles of Nuclear Magnetism* (Oxford University Press, 1961).
22. G. V. H. Wilson, J. A. Barclay, and C. G. Don, *Phys. Rev. B* **6**, 729 (1972).
23. J. Boysen and W. D. Brewer, submitted to *Nucl. Instr. Meth.*
24. J. R. Sites, H. A. Smith, and W. A. Steyert, *J. Low Temp. Phys.* **4**, 605 (1971).
25. M. Prosch and E. Klein, Freie Universität Berlin, private communication (1976).
26. J. Neumann and E. Klein, unpublished (1975); E. Hagn and G. Eska, in *Proc. Int. Conf. on Hyperfine Interactions, Uppsala, 1974*, E. Karlsson and R. Wäppling, eds. (Almqvist and Wicksell, Stockholm), p. 148.
27. R. J. Holliday and W. Weyhmann, *Phys. Rev. Lett.* **25**, 243 (1970).
28. (a) F. Bacon, Ph.D. Thesis, Berkeley, 1972 (unpublished); G. Kaindl, F. Bacon, and D. A. Shirley, *Phys. Rev. C* **8**, 315 (1973); (b) G. Eska and E. Zech, reported at EPS Study Conf. on Nuclear Orientation, Oxford, 1976.
29. J. A. Barclay, private communication (1976).
30. N. J. Stone, private communication (1975).
31. P. T. Callaghan, W. M. Lattimer, and N. J. Stone, in *Proc. Int. Conf. on Hyperfine Interactions, Uppsala, 1974*, E. Karlsson and R. Wäppling, eds. (Almqvist and Wicksell, Stockholm), p. 272.
32. W. D. Brewer and M. Kopp, Int. Meeting on Hyperfine Interactions, Leuven, 1975; *Hyperfine Interactions* **2**, 299 (1976).
33. I. Berkes, R. Haroutunian, and R. Marest, reported at the EPS Study Conf. on Nuclear Orientation, Oxford, 1976.
34. M. Hansen, ed., *Constitution of Binary Alloys* (McGraw-Hill, New York, 1958) and later supplements.
35. A. Narath, K. C. Brog, and W. H. Jones, Jr., *Phys. Rev. B* **2**, 2618 (1970); A Narath, *Phys. Rev. B* **13**, 3724 (1976).
36. J. G. Pérez-Ramirez, L. K. Thomas, and P. Steiner, *J. Low Temp. Phys.* **26**, 83 (1977).
37. I. Berkes, remarks at EPS Study Conference on Nuclear Orientation, Oxford, 1976.
38. W. M. Lattimer, private communication (1974).
39. M. Kopp and W. D. Brewer, in *Proc. 14th Int. Conf. Low Temp. Phys.*, M. Krusius and M. Vuorio, eds. (North-Holland, Amsterdam, 1975), Vol. 4, p. 56; M. Kopp and W. D. Brewer, submitted to *Hyperfine Interactions.*

40. J. A. Cameron, I. A. Campbell, J. P. Compton, R. A. G. Lines, and G. H. V. Wilson, *Proc. Phys. Soc.* **90**, 1089 (1967).
41. C. Sauer, *Z. Phys.* **222**, 439 (1969); A. Heidemann, G. Kaindl, D. Salomon, H. Wipf, and G. Wortmann, *Phys. Rev. Lett.* **36**, 213 (1976); D. Salomon, W. Wallner, and P. West, in *Mössbauer Effect Methodology, Vol. X* (Plenum, New York, to be published).
42. Y. Koi, M. Kawakami, T. Hihira, and A. Tsujimura, *J. Phys. Soc. Japan* **33**, 267 (1972).
43. R. E. Sheriff and D. Williams, *Phys. Rev.* **82**, 651 (1951).
44. L. E. Drain, *Metall. Rev.* **12**, 195 (1967); K. Lüders and Z. Szücs, Berlin, private communication (1975).
45. D. C. Creagh, S. G. Bailey, and G. V. H. Wilson, *Phil. Mag.* **32**, 405 (1975).
46. G. Kaindl, F. Bacon, H.-E. Mahnke, and D. A. Shirley, *Phys. Rev. C* **8**, 1074 (1973).
47. A. Narath and D. C. Barham, *Phys. Rev. B* **7**, 2195 (1973).